FROM THE RADIATION PHYSICS DEPARTMENT (DIRECTOR: ASSOC. PROF. KURT LIDÉN), AND THE ROENTGENDIAGNOSTIC DEPARTMENT (DIRECTOR: PROF. OLLE OLSSON), UNIVERSITY HOSPITAL, LUND, SWEDEN.

DETERMINATION OF INTEGRAL ABSORBED DOSE FROM EXPOSURE MEASUREMENTS

by

CARL CARLSSON

The integral absorbed dose (for brevity the term 'absorbed' will usually be omitted) is defined as the mass integral of the absorbed dose, integrated over the total body, or simply as the energy absorbed by the body during radiation treatment or examination:

$$\Sigma = \int_M D \, dm \tag{1}$$

where Σ is an integral absorbed dose, D absorbed dose, M the total mass, and dm is a mass element.

If the mass is measured in gram and the absorbed dose in rad, the integral dose will be expressed in g·rad units: 1 g·rad = 100 erg = 10^{-5} joule.

(The names and symbols for radiation quantities and units used in this work have been chosen according to ICRU: 'Radiation quantities and units'1962.)

According to the definition, the integral dose can be computed from measurements of the absorbed dose by several detectors uniformly spread throughout the body. This measurement naturally cannot be performed in man, but with a convenient phantom this and other methods can be used to calibrate an external measuring instrument. A large plane-parallel ionization chamber is often used (REINSMA 1962, ARNAL & PYCHLAU 1961, ZIELER 1960, CARLSSON). The chamber is placed between the adjustable diaphragm of a roentgen tube and the patient and measures in the absence of a scattering medium the product

Submitted for publication 3 January 1963.

of the exposure in air and the field area (more exactly the field integral of the exposure in air).

Methods for calculating integral doses from known exposure and field area have been derived by many authors. MAYNEORD (1940) attacked the problem in two ways: first by depth-dose measurements in a phantom and secondly by calculating the incident radiation energy from known energy absorption coefficients for air and measured values of the exposure and field area. In the following, these two methods will be further analyzed.

I. Calculation of integral absorbed dose from depth-dose measurements

Measurements according to the definition of the integral dose have been made by MAYNEORD & CLARKSON (1944). They determined integral doses in a man-equivalent phantom built of wax and rice, in which several ionization chambers were placed. BOAG (1945) used a man-shaped phantom, the celluloid man. This consists of several plane-parallel ionization chambers in which the electrodes also function as phantom material. The same phantom was also used by BEWLEY et coll. (1959) in determining the integral doses from 200 kV and 8 MV radiation. The celluloid man obviates the time-consuming work of constructing isodoses or adding many products of mass and absorbed dose. Instead one has, among other things, to correct for the different incidence angles of the radiation (because of the lamination) and for the fact that the wall material (cellulose acetate) in the ionization chambers causes the sensitivity of the chamber to decrease at the lowest HVT (1 to 4 mm Al) which are of interest here. Chemical dosemeters are very satsifactory from the point of view of the definition integral but their applications are restricted considerably as they suffer from one or more of the following disadvantages: low sensitivity, great energy dependence, especially for low energy roentgen radiation, and rigorous demands on the purity of the chemicals and vessels used.

To measure on the basis of eq. 1, as the cited authors have done, is free from objections in principle but is so laborious that one hesitates to use such a method to calibrate an outer detector for various filters, tube potentials, wave forms, field areas, and focus-skin distances, especially as the uncertainty in the determination of the low dose rates outside the geometrical radiation beam can easily be great. As the dimensions of the phantom used do not correspond to all cases where determinations of integral doses are of interest, the above-mentioned measurements had to be made with many different phantoms.

The energy losses in lateral scattering are relatively small (ZIELER 1961). According to BEWLEY et coll. (1959) they reach about 8 per cent of the incident energy at a HVT of 1.8 mm Cu and a field diameter of 10 cm, if the phantom is a 23 cm high truncated water-cone with a smallest diameter of 25 cm. They estimate the back-scattered and the transmitted energies as 19 and 17 per cent,

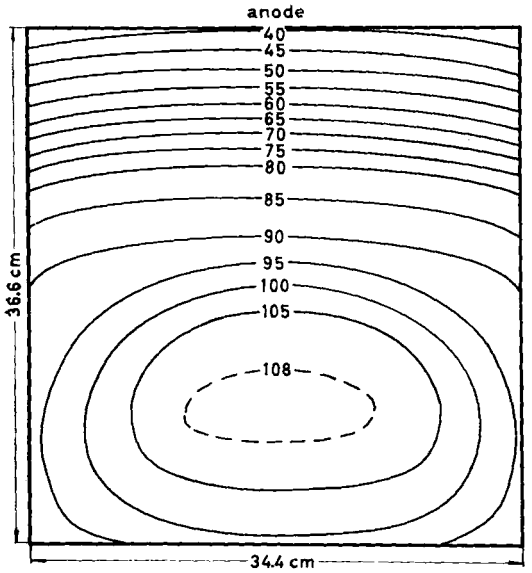

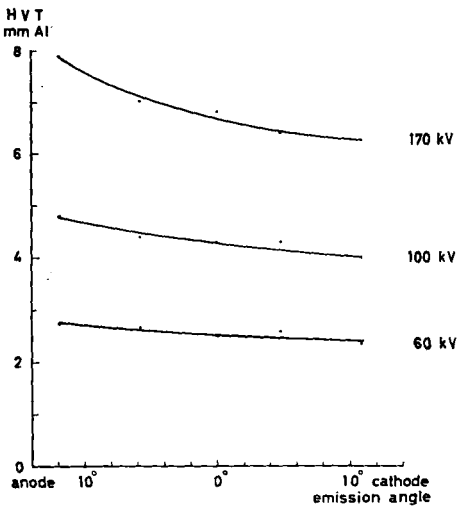

Fig. 2

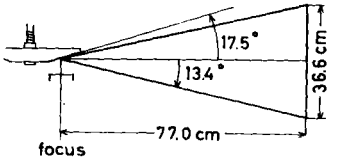

Fig. 1 (left). Measured values for exposure in air from a diagnostic roentgen tube; 75 kV and HVT = 4.3 mm Al.

Fig. 2. Variation of HVT with emission angle from a diagnostic roentgen tube.

respectively. If this phantom is replaced by a water slab of the same thickness but with an infinite lateral extent, one part of the radiation losses through the sides of the cone will after multiple scattering processes in the slab appear as back-scattered or transmitted radiation, and the deviation will be less than the above-mentioned 8 per cent. The deviation will be still less at low HVT, or if the edges of the field are more distant from the lateral limits of the phantom than in the above-mentioned example (this is generally valid in the longitudinal direction of the body when the trunk is irradiated). This idealized phantom (the water slab) opens the way to simplified calculations of the integral dose via central axis depth-dose data and makes simple comparisons between different calculation methods possible. The thickness of the slab is of course easily variable. The well-known approximate formula of MAYNEORD (1940) estimates the integral dose via central axis depth-dose data and integration over the geometrical beam. The drawbacks of this method may be overcome by always choosing the depth-dose values for the calculations from very large fields (the saturated scatter method), independent of the size of the topical fields (HAPPEY 1940 and 1941, LOEFFLER 1956, SCARPA 1960). To elucidate this latter method we may consider a small roentgen pencil, which is a part of and in the centre of

a large, uniform beam, incident on a large phantom. The field is so large that a further enlargement does not affect the central-axis depth doses. The contribution from the small pencil to the integral dose is easily calculated by integrating the dose over that mass which is enclosed by the geometrical limitation of the pencil, as the energy that is lost by photons scattered out of this volume is just compensated by photons scattered in. If instead the same pencil alone irradiates the phantom, it will of course cause the same integral dose but this will be strongly underestimated by integrating the central-axis depth doses over the mass within the volume of the pencil. The mass integral of the dose must instead be extended over the whole phantom to give the same result.

As, owing to radiation quality and phantom thickness, very large fields are often required to assure saturation of the scattered radiation at greater depths, it may be difficult to use the method. MEREDITH and NEARY (1944) have proposed a method of constructing isodose curves which makes it possible to extrapolate depth doses to infinite field areas. The method has only been applied for radiation qualities used in conventional roentgen therapy, and data are lacking for its application with radiation qualities common in diagnostic radiology. TROUT et coll. (1952) have measured central-axis depth doses for radiation qualities with HVT in the region 0.7 to 4.8 mm Al. These measurements were performed with a field having the dimensions 36×43 cm^2. Field dimensions and radiation qualities give rise to the presumption that these measurements could be used for calculating integral doses according to the saturated scatter method. However, it should be pointed out that the exposure rate from a lightly filtered diagnostic tube with small anode angle is far from homogenous over the whole field. An example of measurement of the distribution of the exposure in air from a diagnostic tube is shown in Fig. 1. The field dimensions and focus-skin distance are about the same as given by TROUT. Apparently the exposure varies in the field by more than a factor of two. The integral $\int_A X\,dA$ of the exposure, X, over the field area, A, calculated from Fig. 1 is 13 per cent less than if the whole field had been irradiated with the exposure of the central ray. With the aid of depth-dose data for different field areas the dose contributions from scattered radiation from different parts of the field to the doses of the central ray can be calculated. From this it is possible to compute the effect of the exposure variations of the field on the doses of the central ray.

The integral doses calculated from central-axis depth doses for an inhomogenous field (Fig. 1) and for a homogenous field with the same central-axis dose at zero depth and with the same radiation quality have been compared; the calculated integral dose for the inhomogenous field is only about 3 to 4 per cent below that for the homogenous field. If consideration is taken of the fact that the radiation quality also depends on the direction, the difference will be still less. Fig. 2 shows how the HVT varies with the direction of the radiation along the axis of the roentgen tube, as measured by the author. Another serious

objection to using these depth-dose measurements is that they have been made with a large ionization chamber (the Victoreen thimble chamber). The insertion of an air volume in the phantom material causes an increase in measured exposure because of the decreased filtration of both the primary and scattered radiation but also a diminished exposure contribution because of the elimination of scattered radiation from the displaced volume. This volume effect of the ionization chamber may lead to corrections in the measured depth-doses by several per cent (LIDÉN 1961, SKÖLDBORN 1959). Usually a large ionization chamber causes an overestimate of the depth doses as well as of the integral dose calculated from them. The effects of an inhomogenous field and a large ionization chamber may to a great extent cancel each other.

From the experimental values of TROUT et coll. the author has calculated integral doses as follows:

$$\Sigma = \int_M D dm = \int_0^d \bar{f} X \varrho A_x dx = \bar{f} \varrho A_0 \int_0^d X \left(\frac{F+x}{F}\right)^2 dx \tag{2}$$

where f = f-factor = the ratio between the absorbed dose and the exposure for monoenergetic photons in water.

$\bar{f}$ = the average value of the f-factor for the photon spectrum in the phantom. The values of $\bar{f}$ have been taken from National Bureau of Standards Handbook 78 (1961) and are given in Table 1

X = the exposure in the central ray at the depth x

ϱ = the density of the phantom material

A_0 = surface area of the field, A_x = the field area at the depth x

F = focus—skin distance

x = the depth in the phantom.

If X is expressed as a fraction of the exposure measured in the centre of the beam at the position of the phantom surface but with the phantom removed, if A_0 is chosen as 1 cm², and if the phantom material has the density 1 g/cm³, eq. 2 may be simplified to

$$\Sigma' = \bar{f} \int_0^d X \left(\frac{F+x}{F}\right)^2 dx \, g \cdot \mathrm{rad}/(\mathrm{cm}^2 \cdot \mathrm{R}) \tag{3}$$

This integral has been evaluated for d = 20 cm for fifteen cases with HVT between 0.91 and 4.8 mm Al. The results are presented in Table 1 in the column $\int_0^{20}$. For the calculation of X according to the method of MEREDITH & NEARY, the contribution from the primary radiation has been taken from depth-dose values for zero area ('Depth Dose Tables for Use in Radiotherapy' 1961) and the saturated scatter from HORSELEY & ASPIN (1956).

As earlier, the integral

$$\Sigma' = \bar{f} \int_0^d (P+M) \left(\frac{F+x}{F}\right)^2 dx \tag{4}$$

was determined graphically (the results being given in Table 1 for d = 20 cm); P = exposure from the primary radiation; M = saturated scatter; both are expressed as fractions of the primary exposure at zero depth.

Eqs 3 and 4 are approximately independent of the focus-skin distance. For a semi-infinite phantom, the integral dose per cm² and R will be slightly less for a shorter focus-skin distance (even if the exposure is constant over the whole surface), owing to the fact that the backscattered energy increases with the obliquity of the incident rays (BERGER & RASO 1960).

Table 1

Integral dose and fractional transmission calculated from depth dose values

	kV	Added filter mm	HVT measured mm	$\int_0^{20}$	$\int_0^{\infty}=\Sigma'_{\infty}$	T_{20}	Σ'_{10}	Σ'_{15}
				g·rad·cm^{-2}·R^{-1}				
TROUT et coll	85	0 Al	0.91 Al	4.9	5.0	0.1	4.2	4.7
	85	0.5 Al	1.35 Al	6.0	6.0	0.2	4.7	5.5
	85	1.0 Al	1.54 Al	6.9	7.2	0.3	5.5	6.5
	85	2.0 Al	1.95 Al	8.2	8.6	0.5	6.3	7.5
	85	3.0 Al	2.50 Al	9.2	9.8	0.8	7.0	8.3
TROUT et coll	100	0 Al	1.00 Al	6.7	7.2	0.7	4.9	6.0
	100	0.5 Al	1.60 Al	7.7	8.2	0.7	5.7	6.9
	100	1.0 Al	1.95 Al	8.9	9.6	0.9	6.5	7.9
	100	2.0 Al	2.90 Al	10.6	11.8	1.5	7.4	9.2
	100	3.0 Al	3.60 Al	11.9	13.2	1.6	8.1	10.3
TROUT et coll	130	0 Al	1.20 Al	7.4	7.9	0.6	5.3	6.6
	130	0.5 Al	1.95 Al	9.3	10.3	1.2	6.4	8.0
	130	1.0 Al	2.90 Al	10.8	12.1	1.7	7.2	9.2
	130	2.0 Al	4.1 Al	12.4	14.1	2.1	8.1	10.6
	130	3.0 Al	4.8 Al	13.6	16.2	3.2	8.4	11.2
MEREDITH-NEARY	—	—	0.5 Cu	17.3	21.1	4.8	9.6	13.7
	—	—	1.0 Cu	20.4	26.6	7.6	10.1	15.3
	—	—	2.0 Cu	20.9	28.2	9.1	9.6	15.2
	—	—	3.0 Cu	20.2	28.7	10.6	8.8	14.2
	—	—	4.0 Cu	18.8	27.8	11.3	7.8	12.8

Σ'_d means integral dose per cm^2 and R in a d cm thick water slab. $\int_0^d$ means $\int_0^d \bar{f}X\left(\frac{F+x}{F}\right)^2 dx$. See eqs (3) and (4).

The results Σ' are corrected for errors in depth doses owing to the fact that they are measured in a phantom thicker than d cm. T_d means energy transmitted per incident cm^2 and R

$\frac{T_d}{E_f}$ means fraction of the incident energy which is transmitted through a d cm thick water slab.

In a water slab with finite thickness the transmission decreases with shorter focus-skin distance owing to the longer path in the phantom. These phenomena are however of small importance at ordinary focus-skin distances, and as they mainly refer to the boundary rays they have only a small effect on the central-axis depth doses and the integral dose calculated from them.

Therefore eqs 3 and 4 may be evaluated most easily with depth doses measured as tissue-air ratios. The tissue-air ratio is independent of the focus-skin distance and equivalent to the infinite focus-skin distance in eqs 3 and 4 (JOHNS et coll. 1958).

Fig. 3 gives for roentgen radiation of HVT = 0.5 mm Cu the central-axis

Table 1 *(cont.)*

Σ'_{20}	Σ'_{25}	Σ'_{30}	$\frac{T_{20}}{\Sigma'_{\infty}}$	$\frac{T_{10}}{E_f}$	$\frac{T_{15}}{E_f}$	$\frac{T_{20}}{E_f}$	$\frac{T_{25}}{E_f}$	$\frac{T_{30}}{E_f}$	A_{E_0}	$\bar{f}$
$g \cdot rad \cdot cm^{-2} \cdot R^{-1}$										rad/R
4.9	5.0	5.0	0.018	0.13	0.04	0.014	0.004	0.001	0.23	0.932
5.8	5.9	6.0	0.034	0.16	0.07	0.026	0.010	0.004	0.23	0.932
6.9	7.0	7.1	0.046	0.18	0.08	0.035	0.016	0.007	0.23	0.932
8.1	8.4	8.5	0.053	0.21	0.10	0.048	0.023	0.011	0.23	0.932
9.0	9.4	9.6	0.078	0.22	0.12	0.060	0.031	0.016	0.23	0.932
6.6	6.9	7.0	0.091	0.24	0.13	0.070	0.037	0.020	0.24	0.932
7.6	7.9	8.1	0.084	0.24	0.13	0.064	0.032	0.017	0.24	0.932
8.7	9.2	9.4	0.091	0.25	0.13	0.069	0.036	0.018	0.24	0.932
10.3	10.9	11.3	0.13	0.28	0.17	0.10	0.058	0.035	0.24	0.932
11.6	12.3	12.7	0.12	0.29	0.16	0.090	0.050	0.028	0.24	0.932
7.3	7.6	7.8	0.08	0.25	0.13	0.06	0.028	0.013	0.24	0.932
9.0	9.6	9.9	0.12	0.29	0.17	0.09	0.050	0.027	0.24	0.932
10.5	11.2	11.6	0.14	0.31	0.18	0.10	0.059	0.034	0.24	0.932
12.0	12.8	13.3	0.15	0.32	0.19	0.11	0.068	0.040	0.24	0.932
13.0	14.1	14.8	0.20	0.36	0.23	0.15	0.098	0.063	0.24	0.932
16.3	18.0	19.1	0.23	0.41	0.26	0.17	0.11	0.07	0.25	0.94
18.9	21.3	23.0	0.29	0.47	0.32	0.22	0.15	0.10	0.25	0.95
19.1	21.8	23.7	0.32	0.49	0.34	0.24	0.17	0.12	0.25	0.95
18.1	21.0	23.0	0.37	0.53	0.39	0.28	0.21	0.16	0.23	0.96
16.5	19.3	21.5	0.41	0.57	0.43	0.32	0.24	0.18	0.21	0.96

depth exposure X, expressed as a fraction of the incident exposure in air and multiplied by the factor $\left(\frac{F+x}{F}\right)^2$, as a function of the depth in water. The expression $\left(\frac{F+x}{F}\right)^2 dx$ constitutes a volume element with the incident area = 1 cm². The integral $\int_0^d \bar{f} \cdot X \left(\frac{F+x}{F}\right)^2 dx$ expresses a volume dose. Multiplication by the density of the phantom gives the integral absorbed dose per cm² and roentgen unit according to eq. 3.

According to the saturated scatter method the integral dose will be underestimated if the central-axis depth doses do not have a saturated contribution of scattered radiation. The upper curve in Fig. 3, which was calculated according to MEREDITH & NEARY (infinite field area), meets the saturation conditions, and the area beneath the curve is a measure of the integral dose. The other curves, which refer to depth doses from finite fields, underestimate the integral dose to an increasing extent as the field area and thus the contribution

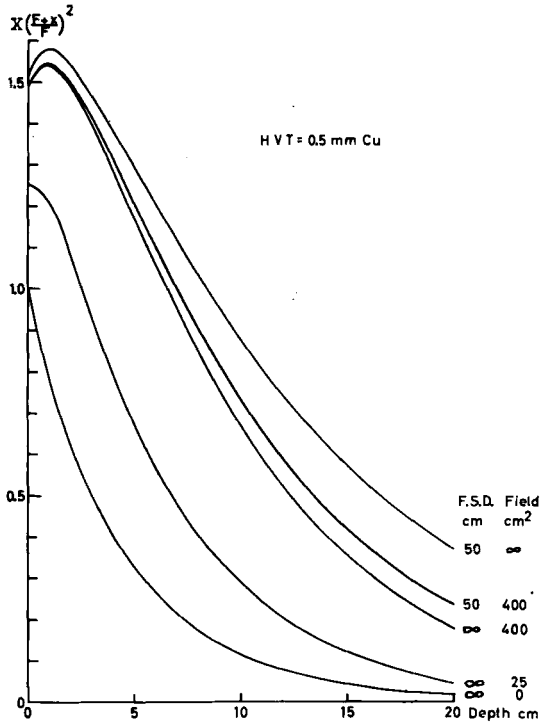

Fig. 3. The integrand in eqs (3) and (4). Upper curve represents depth doses with a saturated scatter contribution. The area beneath this curve is proportional to the integral dose. For doses from a decreasing field area, eq. (3) underestimates the integral dose to an ever increasing extent.

of scattered radiation to the measured depth doses gradually decreases. In succession from top to bottom the different areas beneath the curves underestimate the integral dose by 12, 17, 53, and 75 per cent. Calculations of the integral dose based on depth-dose values and integration over the geometrical cone of radiation can easily result in errors of a factor 2, and in extreme cases even a factor 4, if the saturation conditions are not fulfilled.

Of the two cases in Fig. 3 with the same incident area (400 cm²) but different focus-skin distances (50 cm and infinity), the field with the shorter focus-skin distance best meets the saturation conditions since the field area in this case increases with the depth and the relative contribution of scattered radiation to a point at a depth x is dependent of the area of the field at this depth and is independent of the divergence of the radiation (JOHNS et coll. 1958). MAYNEORD's well-known and often applied formula differs from eq. 3

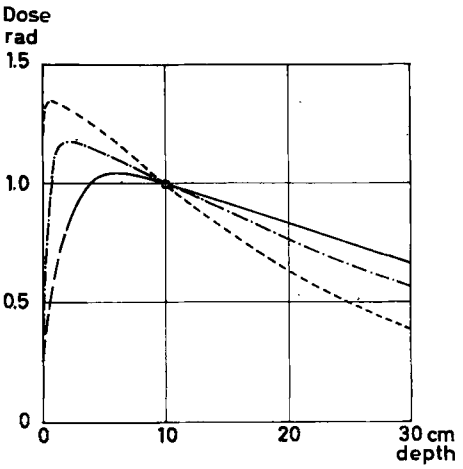

Radiation	Field cm²	Σ'_{20}/D_{10} g·rad·cm^{-2}·rad^{-1}	Σ'_{30}/D_{10}
— 31 MV	50	92	130
-.- 8 MV	400	98	131
--- ^{60}CO	400	101	126

Fig. 4. Ratio of integral dose to tumour dose for three radiation qualities.

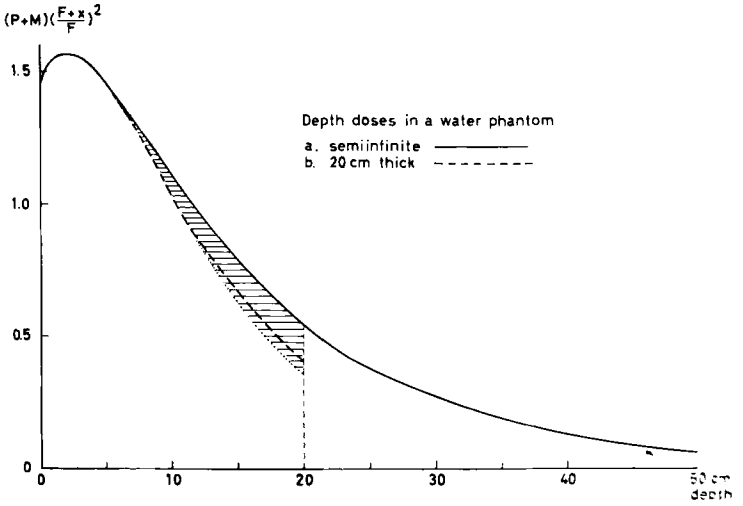

Fig. 5. Depth doses in a semi-infinite medium and in a 20 cm thick water slab. The crossed area corresponds to the energy scattered backwards through the 20 cm plane in the semi-infinite medium. Of this energy a fraction is scattered forward over the same plane, and so on. The broken curve gives the depth doses in the slab.

in the approximation of the depth dose as exponentially decreasing in order to obtain a definition integral which can be evaluated.

This and similar methods therefore underestimate the integral doses in the same way as the graphical method presented here. This graphical method has besides greater accuracy the advantage of being easily applicable to high-energy radiation where the dose is far from exponentially decreasing. For particle as well as photon radiation of sufficiently high energy the forward scattering dominates to the extent that saturation of the central axis depth doses will be reached for the moderate field areas reported in the standard tables. Fig. 4 gives a comparison of integral doses from ^{60}Co, 8 and 31 MV roentgen radiation for the same tissue (tumour) dose at a depth of 10 cm. The dose values have been taken from tables for infinite focus-skin distance ('Depth dose tables for use in radiotherapy', 1961). It is seen that the 31 MV radiation gives the lowest and ^{60}Co the highest integral dose for a 20 cm thick phantom. For a 30 cm thick phantom and the same tumour depth the ^{60}Co radiation is preferable.

As the phantom used for the depth dose measurements is usually semi-infinite, or at least 30 cm deep, the measured depth doses will be larger than if they had been measured in a phantom with smaller dimensions. This is because one part of the dose contribution in the measurement in the thicker phantom originates from radiation that has been back scattered from deeper parts of the phantom. If the integrand $\bar{f}X\left(\frac{F+x}{F}\right)^2$ is extrapolated to infinite depth, i. e. by supposing the whole expression to be exponentially decreasing, and then integrated graphically, first over the actual depth 0-d, and secondly integrated numerically from d to infinity, then the integral dose to the depth d, calculated in this way, can be corrected by considering the energy albedo. The energy albedo A_E is defined as the ratio between the reflected and the incident energy. Albedo values for semi-infinite media of different materials have been calculated by the Monte Carlo method (BERGER & RASO 1960) for photon energies between 20 keV and 2 MeV and different incidence obliquities.

Fig. 5 gives one example of the integrand in eq. 4 in a semi-infinite phantom (solid curve). The broken line refers to the same integrand measured in a phantom d cm thick. In the figures, d has been chosen as 20 cm because this thickness corresponds well with the mean value of the thickness of the trunk in the antero-posterior direction in adults. Of the energy T_d, which is transmitted in a phantom of thickness d, the fraction A_{E1} is reflected if the depth of the phantom is increased to infinity. However, the fraction A_{E2} is backscattered from the first d cm of the phantom, and so on. A_{Ei} is the mean energy albedo value determined from the energy and direction of the photons.

For the calculation of the transmitted energy T_d, in a water slab of thickness d, from dose values measured in a semi-infinite phantom, eq. 5 is valid (for brevity the integrand from eqs 3 and 4 is omitted):

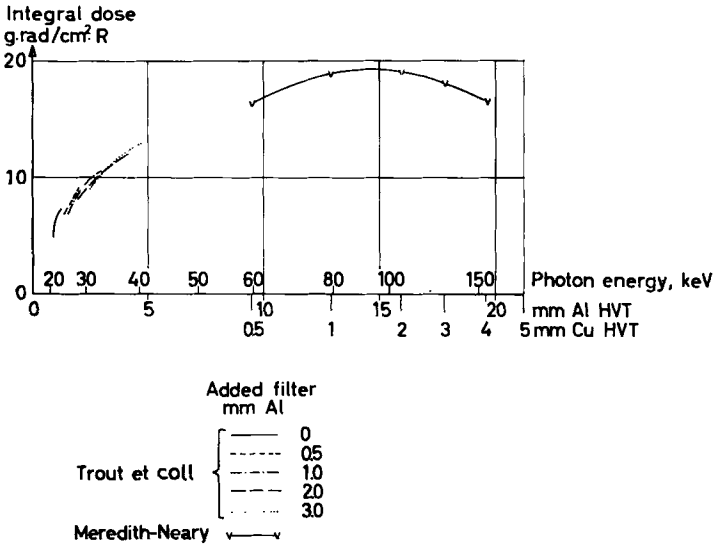

Fig. 6. Calculated integral doses in a 20 cm thick water slab as a function of the HVT in mm Al.

$$\int_d^\infty = T_d - A_{E1}T_d + A_{E2}A_{E1}T_d - A_{E3}A_{E2}A_{E1}T_d + \ldots \tag{5}$$

This series converges rapidly because A_{Ei} as a rule is smaller than 0.3. In the calculations, all A_{Ei} have been chosen equal to $A_{Ei} = A_E = 0.25$. This gives

$$\int_d^\infty = T_d \sum_{n=0}^{\infty} (-A_E)^n, \text{ or } T_d = (1+A_E)\int_d^\infty \tag{6}$$

The corrected integral dose is then

$$\Sigma'_d = \Sigma'_\infty - T_d \tag{7}$$

Eqs 6 and 7 have been solved for different d and are shown in Table 1. The transmission is there expressed as a fraction, partly of the integral dose in a semi-infinite phantom $\left(\frac{T_d}{\Sigma'_\infty}\right)$, and partly of the incident energy $\left(\frac{T_d}{E_f}\right)$. The transmitted and incident energies are here normalized to 1 cm²·R incident. The incident energy fluence per roentgen unit [erg/(cm²·R)] is obtained from the relation $\Sigma'_\infty = E_f(1 - A_{E0})$ (8)

where the energy albedo, A_{E0}, of the primary radiation denotes the fraction of energy backscattered from the phantom surface. A_{E0} is obtained from the spectral calculations described under next heading and from Table 1.

On the basis of the values in Table 1, the integral doses in a 20 cm thick phantom are presented in Fig. 6 as a function of HVT in mm Al. The other two

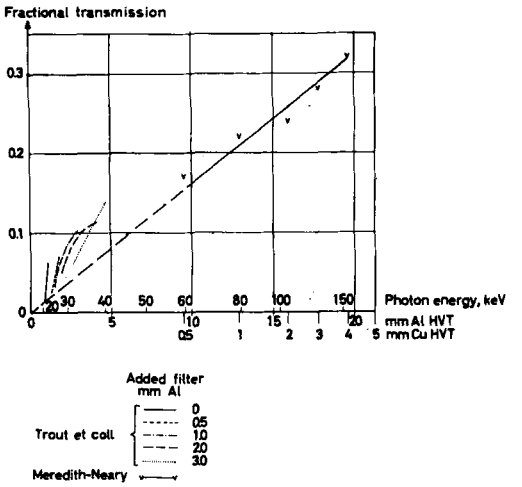

Fig. 7. Fraction of the energy transmitted through a 20 cm thick water slab. The lower the filtration the higher the transmission for low HVT.

scales, HVT in mm Cu and keV, are both related to the first scale in a manner that is valid for monoenergetic photons. Fig. 7 presents in the same way the transmission through a 20 cm thick water phantom. For low HVT a tendency to higher integral dose and transmission can be seen for lightly filtered radiation. This is due to the fact that the HVT in these cases underestimates the average energy of the radiation. We shall return to this question in the following.

II. Calculation of the integral absorbed dose by determination of the incident energy

The incident energy can be measured directly by calorimetric methods. Simultaneous measurement of the exposure allows the determination of the energy fluence necessary to give one roentgen in free air. The expression energy fluence means the time integral of the energy flux density and has the dimension energy per area (ICRU 1962). A calorimetric determination of the energy fluence per roentgen unit with the radiation qualities in which we are interested here has been reported by LAUGHLIN & GENNA (1956). They used roentgen apparatus with potentials between 130 and 400 kV and HVT between 5.1 mm Al and 3.0 mm Cu (see Table 2 and Fig. 8).

Measurements of spectra of primary roentgen radiation, which have been reported by, among others, CORMACK et coll. (1958 and 1960) and HETTINGER & STARFELT (1958) also give the incident energy. These measurements were performed with scintillation spectrometers with various acceleration potentials

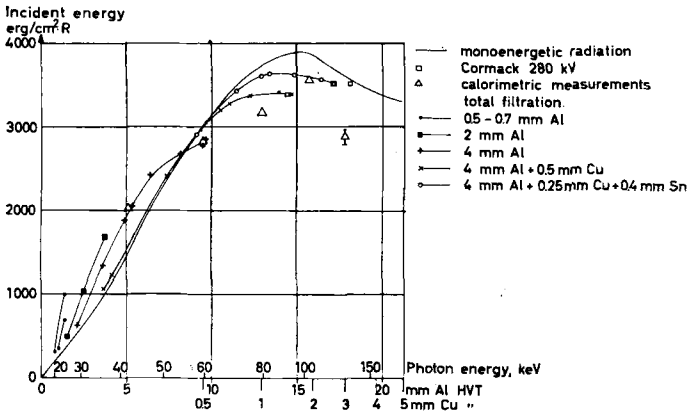

Fig. 8. The energy fluence per R for different filtered radiations as a function of the radiation quality. For 140 kV-radiation with a total filtration of 0.6 mm Al the data for monoenergetic radiation with the same HVT underestimates the incident energy by a factor of 3.

and filters in the roentgen apparatus. Simultaneous measurements of the exposure were not reported, which explains why the experiments do not directly give the energy fluence per roentgen unit. These measurements were performed with a very narrow beam geometry and with intensities so low that exposure measurements under the same conditions would be troublesome.

If the energy absorption coefficients for air and the average energy necessary to produce an ion pair in air are known, the energy fluence per roentgen unit can be calculated from

$$E_f = \frac{W}{\left(\frac{\mu_{en}}{\varrho}\right)_{\text{air}} \cdot 300 \cdot 0.001293} \text{erg} \cdot \text{cm}^{-2}\text{R}^{-1} \tag{10}$$

where E_f is the necessary energy fluence to give 1 R in air, W the average energy dissipated in air to form one ion pair expressed in eV, $\left(\frac{\mu_{en}}{\varrho}\right)_{\text{air}}$ is the mass energy absorption coefficient for air (cm^2/g).

E_f as a function of the photon energy has been calculated by, among others, MAYNEORD (1940), JOHNS & LAUGHLIN (1956), and MULVEY & BALLINGER (1959). The latter in their work use values of the absorption coefficient from WHITE-GRODSTEIN (1957) and their calculations are used in the following. However, 34 eV will be preferred as a value of W instead of the value 33 eV used by MULVEY & BALLINGER (ICRU 1961). As W is assumed to be a constant over the whole energy interval, this involves only a simple correction. Newer values of the energy absorption coefficients (R. T. BERGER 1961) do not appreciably change the results given here.

The incident energy can then be calculated from eq. 10 if the field area and the exposure in air are measured, provided that the photons are monoenergetic. By means of eq. 10, and measured spectra of primary roentgen radiation, the energy fluence per roentgen unit can be calculated for radiation with a continuous spectrum.

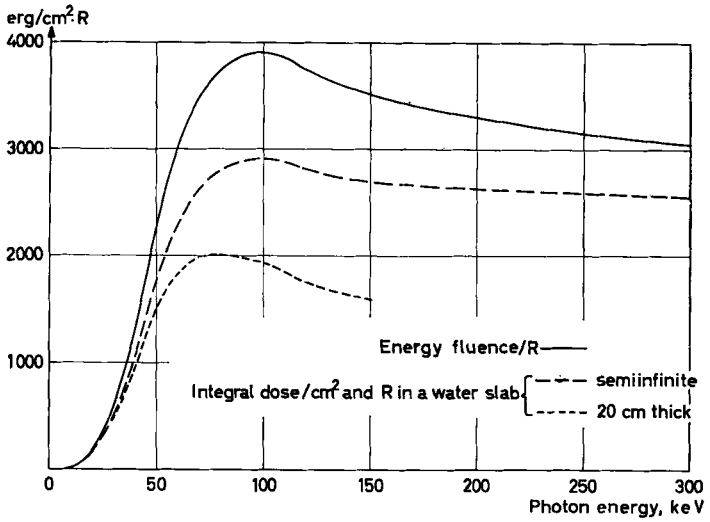

Fig. 9. The incident energy per cm² and R (solid curve) as a function of the photon energy. For the broken curve the reflected energy is subtracted from the incident. For the dotted curve the transmitted as well as the reflected energies are subtracted.

If ε is the energy of the photons, $P(\varepsilon)$ the number of normally incident photons with the energy ε per keV interval and cm², then $P(\varepsilon)\,d\varepsilon$ expresses the number of incident photons per cm² with energies between ε and $\varepsilon + d\varepsilon$; $\varepsilon P(\varepsilon)d\varepsilon$ erg/cm² expresses the energy fluence of these photons;

$\frac{\varepsilon P(\varepsilon)d\varepsilon}{E_f(\varepsilon)}$ expresses the exposure in air which this energy fluence gives.

The mean value of the energy fluence per roentgen unit for the whole spectrum is given by

$$\overline{E}_f = \frac{\int_0^\infty \varepsilon P(\varepsilon)d\varepsilon}{\int_0^\infty \frac{\varepsilon P(\varepsilon)d\varepsilon}{E_f(\varepsilon)}} \tag{11}$$

In the calculation of eq. 11, E_f, as already mentioned, has been taken from MULVEY & BALLINGER with $W = 34$ eV. The spectral distributions were first obtained from measured primary spectra (HETTINGER & STARFELT; CORMACK et coll.) and then by calculating new, more heavily filtered spectra from the first mentioned. Instead of $P(\varepsilon)$, $P(\varepsilon)e^{-\mu(\varepsilon)d}$ is inserted in eq. 11, where $\mu(\varepsilon)$ = the total linear attenuation coefficient for the filter material, d = the linear thickness of the filter; $\mu(\varepsilon)$ has been taken from WHITE-GRODSTEIN (1957). Coherent scattering is also included in $\mu(\varepsilon)$. This is reasonable on account of the extreme narrow-beam geometry in the spectral measurements.

Filter materials and thicknesses have been chosen so that the resulting total

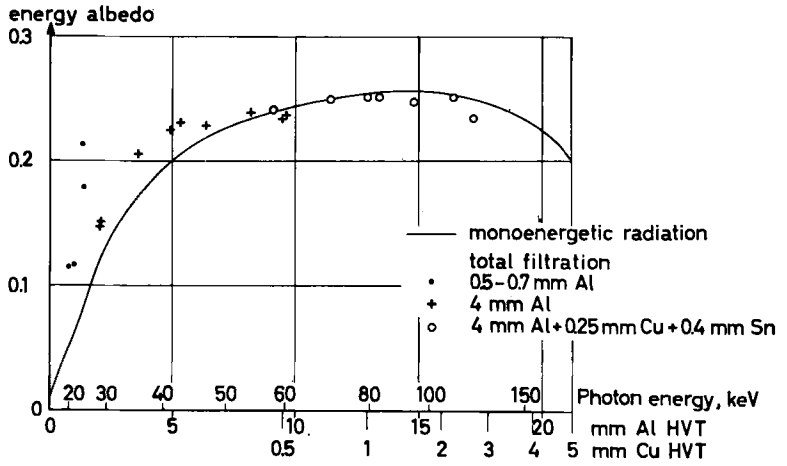

Fig. 10. The energy albedo for monoenergetic photons and for roentgen radiation of different filtration.

filters (inherent and added) amount to 2, 3 and 4 mm Al, 4 mm Al + 0.5 mm Cu, and 4 mm Al + 0.25 mm Cu + 0.4 mm Sn. The calculations cover radiation qualities used both in roentgen diagnostic examinations and in radiotherapy. For each of these spectra, E_f, the energy fluence per roentgen unit, and also the half value thickness or half value layer (HVT or HVL), have been calculated for both mm Al and mm Cu. HVT is here, as in the preceding section, defined as the thickness of an attenuator which is necessary to reduce the exposure or the exposure rate, in air, by a factor of two. In the calculations of the HVT the same absorption coefficients have been used as in the spectral calculations. The HVT is obtained from

$$\frac{1}{2}\int_0^\infty \frac{\varepsilon P(\varepsilon)d\varepsilon}{E_f(\varepsilon)} = \int_0^\infty \frac{\varepsilon P(\varepsilon)e^{-\mu(\varepsilon)\mathrm{HVT}}d\varepsilon}{E_f(\varepsilon)} \tag{12}$$

In practice, instead of HVT, different thicknesses, d, are tried in eq. 12 so that the ratio between the integrals gives values in the neighbourhood of 0.5. Then HVT is obtained by interpolation, i. e. just as in HVT measurements. For measurements of HVT defined as in eq. 12 a stringent narrow-beam geometry is necessary.

Fig. 8. shows both $\bar{E}_f$ and E_f (monoenergetic photons) as functions of HVT in mm Al. The curve without signs corresponds to monoenergetic radiation and the other curves correspond to roentgen radiation with the indicated total filtration. The lowest HVT corresponds to the lowest voltage of the roentgen tube. Specifications of voltages are given in Table 2. As could be expected, the curves for heavily filtered radiation (narrow spectrum) agree best with the curve for monoenergetic photons. The greatest deviations are found with light filtrations and tube voltages of about 100 kV.

Of course the maxima of the curves for the spectra are inferior to that of the monoenergetic radiation. This explains why $\bar{E}_f < E_f$ for HVT greater than 0.5 mm Cu. For low HVT, $\bar{E}_f > E_f$, especially at low filtrations. In this case, for the HVT-measurement of radiation with a broad spectrum, the exposure is reduced to one half mainly by a strong absorption of low energy photons. These low energy photons provide a large contribution to the exposure but a small contribution to the energy fluence, and therefore the spectrum is alloted an effective energy (its HVT) lower than its energy fluence and mean energy would indicate.

From a knowledge of the total filtration the incident energy can be calculated by means of Fig. 8 if the exposure in air and the field area are known. As is seen in Fig. 8, the agreement between the calorimetric measurements of the energy fluence per roentgen unit and the spectral calculations is surprisingly good in the cases where direct comparisons can be made (130 kVp and 4.1 mm Al total filter and 250 kVp and 0.5 mm Al + 1.5 mm Cu total filter). Also in the other cases the same general trends are to be found as in the spectral calculations, i. e. the broader the spectrum the greater the deviations from the monoenergetic curve.

The integral dose is obtained from the incident energy by subtraction of backscattered and transmitted radiation energy.

The fraction of the energy scattered backwards is taken from the energy albedo calculations of BERGER and RASO (1960) and the fraction of the energy transmitted from the calculations in section I. Fig. 9 gives for monoenergetic radiation: (a) the energy fluence per roentgen; (b) the integral dose in a semi-infinite water medium (backscattered energy subtracted from (a); (c) the integral dose in a 20 cm thick water slab (the transmitted energy subtracted from (b)).

The integral doses and the backscattered and transmitted energies in (b) and (c) are per cm^2 and roentgen unit. The transmission calculations are performed for continuous spectra and are not strictly valid for monoenergetic photons. As a further criticism may be mentioned that the backscattered energy from a water slab will be slightly overestimated because it has been calculated for a semi-infinite phantom. According to BERGER & DOGGETT (1956) the reflection from a barrier will rapidly assume its maximum value. A water slab with a thickness of two mean free paths of the primary photons (0.66 MeV) is already equivalent to a semi-infinite medium. LEIMDÖRFER (1963) has shown that to reach the maximum value of reflected energy in concrete a greater thickness in mean free paths is required at lower photon energies in the range 1 to 10 MeV. From backscatter measurements by HETTINGER (1960) it is evident that at least 3 mean free paths are necessary at photon energies as low as between 60 and 100 keV. A mean free path (mfp) in water is for 60 keV photons 4.9 cm and for 200 keV photons 7.3 cm. Then the 20 cm thick water slab is at least 3 to 4 mfp for most of the spectra considered here. The

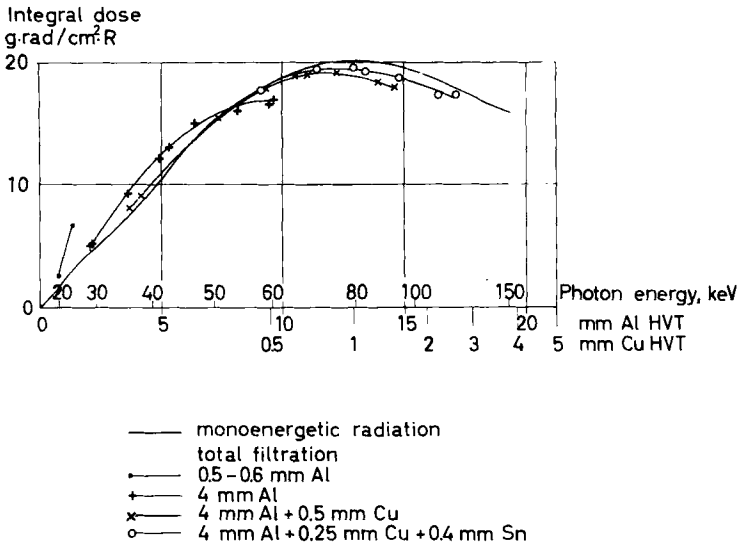

Fig. 11. Integral doses per cm² and R in a 20 cm thick water slab as a function of the radiation quality.

overestimate of the reflection in the calculations is then slight, and only at the highest energies may one expect slightly underestimated integral doses.

For all the spectra in Table 2 a mean energy albedo $\bar{A}_E$ has been calculated as

$$\bar{A}_E = \frac{\int_0^\infty A_E(\varepsilon)\varepsilon P(\varepsilon)d\varepsilon}{\int_0^\infty \varepsilon P(\varepsilon)d\varepsilon} \tag{13}$$

In Fig. 10, both A_E(monoenergetic photons), and $\bar{A}_E$ for the different filtered radiation, are presented as functions of the HVT in aluminium. The reflected and transmitted energies have been subtracted from the incident energy from the different spectra according to

$$\Sigma'_{20} = \frac{\int_0^\infty \{[1-A_E(\varepsilon)]\varepsilon P(\varepsilon) - T_{20}(\varepsilon)\}d\varepsilon}{\int_0^\infty \frac{\varepsilon P(\varepsilon)d\varepsilon}{E_f(\varepsilon)}} \tag{14}$$

The results, integral doses in a 20 cm-thick water slab, are presented in Table 2 and Fig. 11.

III. Comparison between different estimations of integral doses

From Fig. 12, which is a combination of Figs 6 and 11, calculations of integral doses from depth-dose data and primary spectra can be compared. From both methods it is obvious that the HVT-concept measured in mm Al

Table 2

Integral dose calculations from spectral measurements

Spectrum (The term 'calculated' means calculated by the author from the measured spectrum; ~ means alternating voltage.)		kV	Total filtration mm	HVT	
				Calculated	
				mm Al	mm Cu
HETTINGER-STARFELT	measured	45	0.7 Al	1.00	0.030
	calculated	45	2.0 Al	1.50	—
	»	45	3.0 Al	1.80	—
	»	45	4.0 Al	2.04	0.061
	»	45	4 Al+0.5 Cu	3.65	0.13
	»	45	4 Al+0.25 Cu+0.4 Sn	2.06	0.081
HETTINGER-STARFELT	measured	75	0.7 Al	1.35	0.042
	calculated	75	2.0 Al	2.46	—
	»	75	3.0 Al	3.06	—
	»	75	4.0 Al	3.58	0.147
	»	75	4 Al+0.5 Cu	7.33	0.327
	»	75	4 Al+0.25 Cu+0.4 Sn	9.09	0.470
HETTINGER-STARFELT	measured	100	4 Al	4.90	0.193
	calculated	100	4 Al+0.5 Cu	9.3	0.50
	»	100	4 Al+0.25 Cu+0.4 Sn	11.4	0.76
HETTINGER-STARFELT	measured	145	4 Al	6.33	0.306
	calculated	145	4 Al+0.5 Cu	11.0	0.738
	»	145	4 Al+0.25 Cu+0.4 Sn	13.4	1.19
HETTINGER-STARFELT	measured	170	4 Al	8.13	0.46
	calculated	170	4 Al+0.5 Cu	12.2	1.00
	»	170	4 Al+0.25 Cu+0.4 Sn	14.8	1.63
HETTINGER-STARFELT	measured	225	4 Al	9.60	0.68
	calculated	225	4 Al+0.5 Cu	13.9	1.44
	»	225	4 Al+0.25 Cu+0.4 Sn	16.4	2.27
HETTINGER-STARFELT	measured	250	4 Al	9.44	0.686
	calculated	250	4 Al+0.5 Cu	14.6	1.66
	»	250	4 Al+0.25 Cu+0.4 Sn	17.1	2.64
HETTINGER-STARFELT		50~	0.7 Al	0.74	0.022
	calculated	50~	4.0 Al	1.87	0.057
	»	50~	4 Al+0.5 Cu	3.76	0.13
HETTINGER-STARFELT		90~	0.7 Al	1.33	0.04
	calculated	90~	4.0 Al	3.49	0.12
	»	90~	4 Al+0.5 Cu	7.67	0.35

Table 2 *(cont.)*

HVT	Energy fluence per roentgen	Energy albedo per cent	Phantom 20 thick	
Measured mm	erg · cm^{-2}R^{-1}		Transmission per cent	Integral dose per cm^2 and roentgen g · rad · cm^{-2}R^{-1}
	352	11.7	3.4	3.00
—	488	13.3	4.0	4.04
—	562	14.1	4.3	4.60
—	622	14.7	4.6	5.00
—	1 070	18.4	6.8	8.00
—	599	13.7	4.4	4.90
—	690	17.9	5.1	5.15
—	1 030	19.6	9.4	7.30
—	1 200	20.4	10.3	8.30
—	1 340	20.6	10.6	9.30
—	2 410	23.2	12.8	15.4
—	2 910	24.2	15.0	17.7
0.19 Cu	1 880	22.5	13.0	12.1
—	2 970	24.3	15.8	17.8
—	3 440	25.0	18.7	19.4
0.30 Cu	2 420	22.8	15.2	15.0
—	3 280	24.8	17.4	18.9
—	3 650	25.2	22.0	19.2
0.39 Cu	2 670	23.9	16.7	15.9
—	3 370	24.7	18.6	19.1
—	3 630	24.8	24.0	18.6
0.55 Cu	2 850	23.7	17.2	16.9
—	3 420	24.1	22.3	18.3
—	3 580	25.2	26.6	17.3
0.69 Cu	2 770	23.4	17.2	16.5
—	3 390	23.7	23.4	17.9
—	3 520	23.4	27.5	17.3
—	270	10.5	3.1	2.33
—	583	14.1	4.1	4.76
—	1 090	18.6	6.6	8.14
—	670	18.1	8.7	4.94
—	1 360	22.5	9.9	9.20
—	2 520	23.5	13.2	15.9

Table 2 *(cont.)*

Spectrum		kV	Total filtration mm	HVT	
				Calculated	
				mm Al	mm Cu
CORMACK	measured	140	0.6 Al	1.33	0.05
	calculated	140	2.0 Al	3.75	—
	»	140	3.0 Al	4.62	—
	»	140	4.0 Al	5.30	0.23
	»	140	4 Al+0.5 Cu	10.5	0.67
	»	140	4 Al+0.25 Cu+0.4 Sn	12.9	1.10
CORMACK*	measured	140	0,6 Al	1.43	0.05
	calculated	140	4.0 Al	5.42	0.23
	»	140	4 Al+0.5 Cu	10.5	0.67
	»	140	4 Al+0.25 Cu+0.4 Sn	12.9	1.10
CORMACK	measured	280	2 Al+0.25 Cu+0.2 Sn	14.4	1.77
	»	280	2 Al+0.25 Cu+0.6 Sn	17.1	2.62
	»	280	2 Al+0.25 Cu+1.2 Sn	18.1	3.10
EHRLICH	measured	50	0.5 Al	0.77	0.023
	calculated	50	4.0 Al	2.09	0.064
	»	50	4 Al+0.5 Cu	4.14	0.144
	»	50	4 Al+0.25 Cu+0.4 Sn	2.35	0.071
LAUGHLIN	measured	130~	4.1 Al		
calorimeter	»	200~	0.1 Al+0.3 Cu		
	»	250~	0.1 Al+0.35 Cu		
	»	250~	0.5 Al+1.5 Cu		
		400~	1 Al+2.0 Cu		

* In these calculations $\left(\frac{\mu_{en}}{\varrho}\right)_{air}$ in eq. 10 is taken from R. T. BERGER (1961).

does not correspond to a unique integral dose. As in Figs 6, 7, 8 and 11, Fig. 12 shows that the HVT underestimates the average energy of the spectra in the low energy region.

The agreement between the results of the two calculation methods is rather good, although in the low energy region, 1 to 5 mm Al HVT, the depth dose calculations result in higher integral doses than the spectral calculations for the same HVT and filtration. As reasons for the deviations may be mentioned:

1. TROUT et coll. (1952) measured their depth doses with a load up to 500 mA of a full wave, 60 cycle diagnostic roentgen unit, while the spectral measurements were performed with so low currents, less than 1 mA, that the tube voltage owing to the influence of the cable capacitance (TROUT et coll. 1960) was constant. There probably are a relatively greater number of low energy photons in the radiation from a tube with pulsating voltage. This means that

Table 2 *(cont.)*

HVT	Energy fluence per roentgen	Energy albedo per cent	Phantom 20 cm thick	
Measured mm	erg · cm^{-2}R^{-1}		Transmission per cent	Integral dose per cm^2 and roentgen g · rad · cm^{-2}R^{-1}
1.33 Al	995	21.3	12.0	6.63
—	1 680	22.3	13.0	10.9
—	1 890	22.8	13.4	12.1
—	2 050	23.1	13.6	13.0
—	3 200	24.6	16.8	18.8
—	3 620	25.2	21.0	19.5
1.33 Al	1 040	—	—	—
—	2 130	—	—	—
—	3 230	—	—	—
—	3 590	—	—	—
1.77 Cu	3 390	23.8	23.4	17.9
2.63 Cu	3 530	23.5	27.5	17.3
3.14 Cu	3 620	23.2	29.1	17.3
—	302	11.5	3.5	2.57
—	649	15.1	4.7	5.20
—	1 230	19.3	7.4	9.00
—	784	16.8	5.8	6.06
5.1 Al	2 020			
0.5 Cu	2 840			
1.0 Cu	3 170			
1.9 Cu	3 560			
3.0 Cu	2 880 ± 90			

the HVT underestimates to an even greater extent the average energy of the radiation, which may explain the whole deviation. In Table 2, a few spectra with pulsating tube voltage (HETTINGER & STARFELT) have been used for integral-dose calculations. The expected higher integral dose per cm^2 and roentgen unit than for radiation with the same HVT and filtration, but with constant voltage, has not been observed with certainty.

2. The relatively large ionization chamber used by TROUT et coll. gives too high values in a phantom.

3. The spectral measurements underestimate the number of low energy photons. The number of low energy photons $P(\varepsilon)$, just as the energy fluence per roentgen unit $E_f(\varepsilon)$, varies rapidly with the energy, ε, for the lowest energies, which explains the fact that the calculation of eq. 11 is most uncertain for low photon energies.

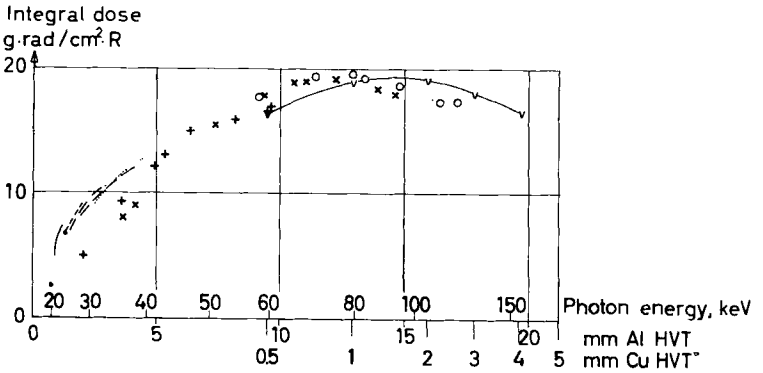

Fig. 12. Combination of figs 6 and 11. The integral doses calculated from depth doses and spectral measurements can be compared.

Integral doses calculated by means of the Meredith-Neary method differ less than those based on TROUT et coll. from the spectral calculations (Fig. 12). The method of Meredith-Neary gives lower integral doses for HVT beneath 1 mm Cu and higher for HVT over 2 mm Cu than the spectral calculations. The low values may be due to an underestimate of the contribution of the saturated scatter to the depth doses by the above-mentioned method. This is indicated by the fact that if the contribution of the saturated scatter is taken from a table for short focus-skin distance, the calculated integral dose will be greater than for a greater focus-skin distance. The integral doses estimated from eq. 3 are greater for a short focus-skin distance because the field area and thus the contribution of scattered radiation is greater for greater depths (JOHNS et coll.). When the scatter contribution is already saturated, one may instead expect the reverse for a short focus-skin distance, as in this case the intensity of the border radiation decreases according to the inverse square law. Increased reflection and inhomogeneities in the field also play a role (Fig. 1).

As the energy albedo has been calculated for a semi-infinite phantom, the reflection will be overestimated to a greater extent for thinner water slabs. This results in an underestimate of the spectral calculations of the integral doses, especially at large HVT. This may be the reason for the lower values of the integral doses, calculated from the spectra, for the higher HVT. It must be admitted however that the calculations of the transmission are so inaccurate that nothing definite may be said concerning these small deviations.

To compare the calculations with those of other authors the results published by SCARPA (1960), KELLER (1956), REINSMA (1962), and ZIELER (1961) have been added in Fig. 13 to the results from Fig. 12. SCARPA uses the saturated scatter method and his results are approximately identical with the results based on the Meredith-Neary method. The calculations of KELLER give

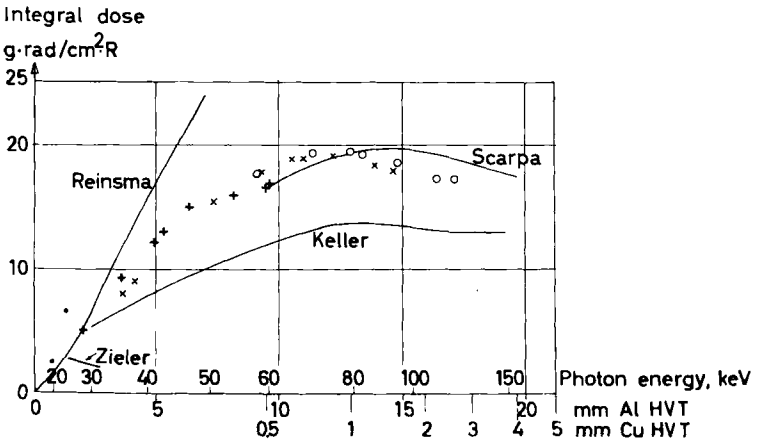

Fig. 13. Integral doses per cm² and R calculated by different authors are added to fig. 12.

appreciably lower results whereas REINSMA simply assumes that all of the incident energy is absorbed. He neglects backscatter and transmission and assumes that the HVT well describes the radiation quality. Neglecting the spectral differences for radiation with the same HVT involves a faulty estimation of the dose-saving effect of the filtration of a roentgen tube. In his measurements of integral doses, properly incident energy, in roentgen diagnostic examinations he uses a roentgen tube with an inherent filtration equivalent to 2 mm Al. He compares measured integral doses without and with an added filter composed of 0.2 mm Cu + 1 mm Al and does not observe any decrease of the integral doses in spite of the fact that the skin doses decrease by a factor of 4 for the heavier filter. The decrease of the integral dose (incident energy) produced by the filter is concealed as he underestimates the incident energy more for the unfiltered radiation than for the filtered. This is evident from Fig. 8 where the HVT varies between 1.5 and 4 mm Al for unfiltered radiation and between 4 and 9 mm Al for filtered radiation.

ZIELER (1961) also calculates integral doses from exposure measurements and energy absorption coefficients for air. Like REINSMA he chooses for this heterogeneous and low energy radiation an average absorption coefficient taken from monoenergetic radiation with the same HVT. On the other hand he estimates the energy loss due to scattering and transmission in various phantoms. He uses the energy flux density (spherical intensity) instead of the energy current density (plane intensity) in his estimate of the reflected and transmitted energies (BEWLEY et coll. 1959, FANO et coll. 1959, WHYTE 1959). The reflected and transmitted energies will then be overestimated by up to a factor 2, which means a grave underestimate of the integral dose.

Acknowledgements

I wish to express my sincere gratitude to Assoc. Prof. Kurt Lidén for continuous encouragement and valuable discussions and to Prof. Olle Olsson for his interest in my work. The investigation was supported by grants from the Swedish Cancer Society and the Swedish Medical Research Council.

SUMMARY

Methods of evaluating integral doses administered in roentgen diagnostics and radiation therapy are analysed. The calculations are performed by using either central-axis depth-dose data with a saturated contribution of scattered radiation, or roentgen radiation spectra, experimentally determined by other authors, and performing necessary corrections for escape energy. The relation between exposure and the incident energy per unit area is calculated for the different spectra by means of energy absorption coefficients for air. Both methods give roughly the same results but disagree with certain published data.

ZUSAMMENFASSUNG

Methoden zur Schätzung der Integraldosen, welche Patienten bei röntgendiagnostischen Untersuchungen und bei Strahlenbehandlungen erhalten, werden analysiert. Zwei Methoden sind hierbei benutzt worden: erstens Anwendung von Tiefendosen des Centralstrahles bei unendlich grossem Feld, und zweitens Anwendung von Röntgenspektren für Bestimmung der einfallenden Energie unter Berücksichtigung der entstehenden Strahlenverluste. Der Zusammenhang zwischen Standard-Ionendosis und der eingestrahlten Energie pro Flächeneinheit ist mit Hilfe von Energieabsorptionskoeffizienten für Luft berechnet worden. Beide Methoden geben etwa dieselben Resultate. Die hier vorgelegten Daten stimmen mit gewissen veröffentlichten Ergebnissen nicht überein.

RÉSUMÉ

L'auteur analyse les méthodes d'évaluation de la dose intégrale reçue par les sujets irradiés par les rayons roentgen. Les doses intégrales ont été calculées à partir des doses en profondeur sur l'axe central avec participation à saturation du rayonnement diffusé et à partir des mesures de spectre de tubes roentgen sous divers voltages et avec divers filtres. Les spectres donnent l'énergie incidente; la dose intégrale est calculée comme la différence entre l'énergie incidente et l'énergie de sortie.

REFERENCES

ARNAL M.-L., und PYCHLAU H.: Die Strahlenbelastung des Patienten bei röntgendiagnostischen Untersuchungen. Fortschr. Röntgenstr. 95 (1961), 323.

BERGER M. J., and DOGGETT J.: Reflection and transmission of gamma radiation by barriers: Semianalytic Monte Carlo calculation. J. Res. Nat. Bur. Stand. 56 (1956), 89.

— and RASO D. J.: Monte Carlo calculations of gamma-ray backscattering. Radiat. Res. 12 (1960), 20.

BERGER R. T.: The X- or gamma-ray energy absorption or transfer coefficient: Tabulations and discussion. Radiat. Res. 15 (1961), 1.

BEWLEY D. K., BATCHELOR A. L., LOWE J. et coll.: Integral doses at 200 kV and 8 MeV. Brit. J. Radiol. 32 (1959), 36.

BOAG J. W.: On the energy absorbed by a patient during X-ray treatment. Brit. J. Radiol. 18 (1945), 235.

CARLSSON C.: Integral absorbed doses in roentgen diagnostic procedures. To be published in Acta radiol.

CORMACK D. V., and BURKE D. G.: Spectral distributions of primary and scattered 140 kVp X-rays. Radiology 74 (1960), 743.

— DAVITT W. E., BURKE D. G., and RAWSON E. G.: Spectral distributions of 280 kVp X-rays. Brit. J. Radiol. 21 (1958), 565.

DEPTH DOSE TABLES FOR USE IN RADIO-THERAPY. Brit. J. Radiol. Suppl. No. 10 (1961).

EHRLICH M.: *In:* ICRU Report 1956. Nat. Bur. Stand. Handbook 62, Washington 1957.

FANO U., SPENCER L. V., and BERGER M. J.: Penetration and diffusion of X-rays. Handbuch der Physik, Bd 38/2. Springer, Berlin 1959.

HAPPEY F.: The integration of radiation dosage and the absorption of energy in tissue for X- and gamma radiation. Brit. J. Radiol. 14 (1941), 235.

— Volume integration of dosage for X- and γ-radiation. Nature 143 (1940), 668.

HETTINGER G.: Angular and spectral distributions of backscatter radiation from slabs of water brass, and lead irradiated by photons between 50 and 250 keV. Acta radiol. 54 (1960), 129.

— and STARFELT N.: Bremsstrahlung spectra from roentgen tubes. Acta radiol. 50 (1958), 381.

HORSLEY R. J., and ASPIN N.: New values of constants for use in calculating isodose curves by the method of Meredith and Neary. Brit. J. Radiol. 29 (1956), 625.

ICRU Report 1959. Nat. Bur. Stand. Handbook 78, Washington 1961.

ICRU Report 10a 1962. Radiation Quantities and Units. Nat. Bur. Stand. Handbook 84, Washington 1962.

JOHNS H. E., BRUCE W. R., and REID W. B.: The dependence of depth dose on focal skin distance. Brit. J. Radiol. 31 (1958), 254.

— and LAUGHLIN J. S.: Interaction of radiation with matter. *In:* G. J. HINE and G. L. BROWNELL: Radiation dosimetry, p. 49. Academic Press, New York 1956.

KELLER H. L.: Die Ermittlung der Raumdosis bei der Röntgenbestrahlung. Fortschr. Röntgenstr. 84 (1956), 73.

— Grundlagen der Raumdosisermittlung bei allen gebräuchlichen Qualitäten der Röntgenbestrahlung. Fortschr. Röntgenstr. 85 (1956), 333.

LAUGHLIN J. S., and GENNA S.: Calorimetric methods. *In:* G. J. HINE and G. L. BROWNELL: Radiation dosimetry, p. 411. Academic Press, New York 1956.

LEIMDÖRFER M.: The backscattering of gamma radiation from plane concrete walls. AE -92, Stockholm 1962.

LIDÉN K.: Errors introduced by finite size of ion chambers in depth dose measurements. *In:* Selected topics in radiation dosimetry, p. 161. International Atomic Energy Agency, Vienna 1961.

LOEFFLER R. K.: A simplified method of estimating integral dose in radiotherapeutic practice. Radiology 67 (1956), 371.

MAYNEORD W. V.: Energy absorption. Brit. J. Radiol. 13 (1940), 235.

— and CLARKSON J. R.: Energy absorption II. Integral dose when the whole body is irradiated. Brit. J. Radiol. 17 (1944) 151, 177.

MCGINNIES R. T.: X-ray attenuation coefficients from 10 keV to 100 MeV. Nat. Bur. Stand. Suppl. to Circ. 583. Washington 1959.

MEREDITH W. J., and NEARY G. J.: The production of isodose curves and the calculation of energy absorption from standard depth dose data. Brit. J. Radiol. 17 (1944), 75, 126.

MULVEY T., and BALLINGER J.: The energy and quantum equivalent of the roentgen. Brit. J. Radiol. 32 (1959), 408.
REINSMA K.: Dosemeters for X-ray diagnosis. Philips Technical Library, Eindhoven 1962.
SCARPA G.: Integral dose and high energy radiation. Brit. J. Radiol. 33 (1960), 770.
SKÖLDBORN H.: On the design, physical properties and practical application of small ionization chambers. Acta radiol. (1959) Suppl. 187.
TROUT E. D., KELLEY J. P., and CATHEY G. A.: The use of filters to control radiation exposure to the patient in diagnostic roentgenology. Amer. J. Roentgenol. 67 (1952), 946.
— — and LUCAS A. C.: Influence of cable length on dose rate and half-value layer in diagnostic X-ray procedures. Radiology 74 (1960), 255.
WHITE-GRODSTEIN G.: X-ray attenuation coefficients from 10 keV to 100 MeV. Nat. Bur. Stand. Circular 583, Washington 1957.
WHYTE G. N.: Principles of radiation dosimetry. John Wiley & Sons, New York 1959.
ZIELER E.: Messung der Strahlenbelastung von Patienten in der Röntgendiagnostik. Fortschr. Röntgenstr. 92 (1960), 211.
— Untersuchungen zur Bestimmung der Integraldosis in der Röntgendiagnostik. Fortschr. Röntgenstr. 94 (1961), 248.